SCITECH
2 RESEARCH ORGANISATION

Volume 3, Issue2
January 20, 2016

Journal of Progressive Research in Chemistry
www.scitecresearch.com

Removing Diethylphthalate (DEP) from Water Systems using Zeolites and Mesoporous Materials

Aoi Masuda[1], Tomohiro Morita[2], Naoki Itayama[1], Youzou Yakushi[3], Masahiko Akiike[3], Tomoki Kawaguchi[3], Hisashi Honda[1,2,3,4*], Shin'ichi Ishimaru[5]

[1]International College of Arts and Sciences, Yokohama City University, Kanazawa-ku, Yokohama, 236-0027, Japan
[2]International Graduate School of Arts and Sciences, Yokohama City University, Kanazawa-ku, Yokohama, 236-0027, Japan.
[3]Faculty of Science, Yokohama City University, Kanazawa-ku, Yokohama, 236-0027, Japan.
[4]Graduate School of Nanobioscience, Yokohama City University, Kanazawa-ku, Yokohama, 236-0027, Japan.
[5]Department of Green and Sustainable Chemistry, Tokyo Denki University, Adachi-ku, Tokyo, 120-8551, Japan.

Abstract

In order to remove diethylphthalate (DEP) molecules from water systems, zeolites of faujasite (FAU), ferrierite (FER), mordenite (MOR), and mesoporous silica (MCM-41) were employed in this study. ^{1}H nuclear-magnetic-resonance (NMR) spectra showed that FAU was effective in eliminating DEP from aqueous solutions. In addition, solid-state ^{1}H NMR spectra with a magic-angle-spinning (MAS) rate of 30 kHz revealed that a larger amount of DEP was adsorbed on FAUs with higher Si/Al ratios. Our NMR spectra also showed that a chemical shift of the signal assigned to water molecules adsorbed on the FAUs is linked to the amount of DEP adsorption. ^{1}H MAS NMR spectra also revealed that DEP molecules prefer to adsorb on the four-membered ring site rather than the canter or/and window of the supercage in FAUs. Since porous materials are frequently present in ground and water systems such as rivers, ponds, and lakes, this study also showed that DEP could adsorb onto soils in aquatic environments and remain in the water system for a long time.

Keywords Diethylphthalate; Zeolite; Faujasite; Ferrierite; Mordenite; Mesoporous Silica; Adsorption; NMR.

1. Introduction

Diethylphthalate (DEP) is a chemically stable, colorless, and flavorless liquid at ambient temperature and barely soluble in water (591 mg·L^{-1}) [1, 2]. It is employed in the chemical industry as a softener in plastics and as a solvent and antifoaming agent in cosmetics. DEP is usually used as an additive in materials. It does not form chemical bonds with the material, and therefore, it can migrate to the external environment from the interior of the products [3-5]. Recent reports show significant concentrations of DEP in the water and sediments of rivers, ponds, sewers, etc. worldwide [6-9]. Toxicological studies report that DEP is considered as a micropollutant since it mimics the behavior of female hormones in animals (endocrine disrupter) [10-12]. DEP is known to be hazardous to human health and stricter quality standards for DEP have been established in the USA, EU, Canada, etc. [2, 13], and effective methods to eliminate DEP from aquatic environments are needed [14]. Several methods of removing DEP from water systems have been investigated, such as adsorption on activated carbon [15-18] and other adsorbents without zeolites [11, 19-24], biological treatment [25, 26], oxidation [27, 28], ozonation [11, 29-31], and hybrid methods [30]. Adsorption on activated carbon is an economical process for the removal of organic compounds. However, the separation of spent carbon causes a loss of carbon or the blockage of filters [32]. Biodegradation is also a low-cost separation method, however, a long time is usually needed to reduce the concentration of pollutants. Oxidation procedures are frequently effective in decomposing phthalates, but the toxicity of the intermediate compounds remains unclear [33]. These methods focus of eliminating DEP molecules

from water systems, however, water is always attached to earth as porous materials such as zeolite are naturally present in the ground.

Several zeolites such as Faujasite-type (FAU), Ferrierite-type (FER) and Mordenite-type (MOR), are obtained from natural soils [34], and they are widely used in chemical industries and scientific studies. The general chemical formula of zeolites in a unit cell is $M_{(x/n)}(SiO_2)_{(192-x)}(AlO_2)_x \cdot yH_2O$, where M is a cation of charge $+n$. The ion M can be exchanged with another cation in aqueous solutions. The number of water molecules (y) in the unit cell depends on the steam pressure. In the case of FAU, the unit framework is constructed of sodalite cages combined to each other by hexagonal prisms, and creates a micro-pore called a supercage. X-ray and neutron diffraction measurements reveal that the positions of the cations are distributed at three sites on the frame [35-38]: Site I is located in the center of the hexagonal prism and in the sodalite cage towards the hexagonal prism, Site II is located in the six-membered ring windows on the sodalite cage, and Sites III' and III are distributed in the center of the twelve-membered ring (window of supercage) and the four-membered ring on the sodalite cage, respectively. It is also known that the cation populations of Site III and III' increase with decreasing Si/Al ratios over a range of Si/Al ratios < 2 [39-42]. The cations located at Site I on the frame can hardly be exchanged by large cations (K^+, Rb^+, Cs^+, etc.) in solutions, because the window diameter of six-rings is approximately 250 pm. However, the cations at Site II, III, and III' can be substituted by mono atomic cations. Since the charge density on the frame is dependent on the amount of Al atoms, FAU with low Si/Al ratios shows hydrophilic characteristics. Solid-state ^{29}Si, ^{27}Al, and ^{1}H nuclear magnetic resonance (NMR) measurements with the magic-angle-spinning (MAS) method reveal the properties of acid sites in FAU as well as determining the Si/Al ratios [43-47]. In addition, high resonance ^{1}H MAS NMR spectra with a MAS speed of 30 kHz and thermogravimetry-differential thermal analysis (TG-DTA) measurements show that water molecules are strongly adsorbed on Li- and Cs-type FAU compared to those in K-type FAU [47]. Since the window diameter of the supercage is ~740 pm, small size molecules e.g. methanol, phenol, toluene, etc. can be reacted in the supercage rather than in the sodalite cages.

In the case of MOR, straight channels with eight- and twelve-membered rings of 260 × 570 and 650 × 700 pm (a cross section of channel is elliptical, therefore, the expression short × long axis length is used), respectively, are inserted parallel to the crystallographic c-axis. These cylindrical channels are interconnected by another eight-ring channel along the b-axis with a size of 340 × 480 pm [48]. MOR is frequently used in the petrochemical catalytic process as well as theoretical and experimental scientific studies [48-52]. Based on these cross-section sizes, medium-sized ions or molecules can diffuse along the crystallographic *c*-axis. A similar framework is constructed in FER: two kinds of straight channel structures with eight-membered (350 × 480 pm) and ten-membered oval rings (420 × 540 pm) [53]. FER is frequently used as a catalyst in alkene isomerization [54-56] and adsorbents for H_2, N_2, CO, CO_2, etc. [57-59]. Contrary to zeolites, mesoporous silica such as MCM-41 can also adsorb organic and inorganic molecules on its inner surfaces and perform catalytic functions. MCM-41 has cylindrical cavities with a uniform diameter of ~1.2 nm. Since MCM-41 shows catalytic and adsorbing characteristics [60-65], it is used widely in chemical industries and scientific endeavors in addition to zeolites.

In this study, we treated 25 types of FAU with Si/Al ratios of 1.0, 1.2, 1.7, 2.4, and 3.5, and cations of Li, Na, K, Rb, and Cs, in order to evaluate the ability to filter DEP in aqueous systems. FER, MOR, and MCM-41 were also employed to compare with FAUs. We obtained ^{1}H MAS NMR spectra with a MAS speed of 30 kHz to reveal adsorption states of DEP molecules on the porous materials. Additionally, porous materials are frequently present in the ground; therefore, understanding the adsorption states of DEP on FAU, FER, and MOR are important for purifying river and lake environments.

2. Experimental

In this study, two commercial FAUs of the Na form (Tosoh) with Si/Al ratio of 1.2 and 2.4 were employed, and three specimens (Si/Al ratio of 1.0, 1.7, and 3.5) were prepared using the same methods previously reported [47]. Ion-exchanged FAUs were also prepared using the same method as described in a previous report [47]. Samples of DEP adsorbed on FAUs were prepared by the following method: FAU was added into an aqueous solution saturated with DEP and stirred at 25°C for 24 h. The FAUs were filtered and dried in ambient conditions. In order to determine the adsorbed states of DEP in FAU, each FAU was immersed in DEP (it is a liquid at room temperature) at room temperature for 24 h. After filtering the specimens, the samples were washed with a small amount of benzene to remove DEP molecules adsorbed on the outer surface of FAU (DEP can dissolve in benzene well). The specimens were dried at ambient temperature. In this study, we treated 25 types of FAU with Si/Al ratios of 1.0, 1.2, 1.7, 2.4, and 3.5, with cations of Li, Na, K, Rb, and Cs. We defined M*x* as M-type FAU with a Si/Al ratio of *x*. In addition, DEP saturated solution and DEP in a liquid state were used; these are defined as DEP(aq) and DEP(l), respectively, e.g. DEP(aq)-Li2.4 is Li-type FAU with a Si/Al ratio of 2.4 prepared by filtering from the DEP saturated solution. FER and MOR were obtained commercially (Wako). MCM-41 was prepared using reported procedures [65]. The same method was used for adsorbing DEP on FER, MOR, and MCM-41.

In order to determine the crystal structures of the samples prepared in this study, powder X-ray diffraction (XRD) measurements were performed using a Bruker D8 ADVANCE diffractometer in steps of 0.02° with a Cu anticathode. Our XRD spectra showed that peaks of the specimens closely match those reported in a previous report [46]. N_2 adsorption isotherms were observed at 77 K using a Bell Japan Inc. BELSORP-mini II. Before the adsorption experiments, all samples were crushed in a mortar and heated at 673 K for 1 h in vacuum. pH values of the DEP saturated solution were measured using a CyberScan pH 510 at room temperature.

^{1}H and ^{29}Si MAS NMR measurements were performed using a Bruker Avance 600 spectrometer (14.10 T) with the MAS accessory. Solid-state high-resolution ^{1}H MAS NMR spectra were recorded at a Larmor frequency of 600.13 MHz with a MAS speed of 30 kHz. Powdered samples and a small amount of silicon powder were packed in a ZrO_2 NMR tube with an outer diameter of 2.5 mm. Here, the silicon powder, EP-2600 (TORAY), is used as the internal reference for ^{1}H chemical shifts (δ = 0.12 ppm). Si/Al ratios were determined by analyzing the ^{29}Si MAS NMR spectra at 119.22 MHz with a MAS speed of 10 kHz. FAUs without adsorbed DEP were packed into a ZrO_2 rotor with an outer diameter of 4.0 mm. All ^{1}H and ^{29}Si spectra were obtained from free-induction-decay (FID) signals, which were recorded after a $\pi/2$ pulse. A pulse sequence of ^{29}Si MAS NMR was designed with a ^{1}H decoupling pulse. Recycle times of 5 and 60 s were employed on ^{1}H and ^{29}Si MAS NMR measurements, respectively. ^{29}Si MAS NMR spectra showed Si/Al ratios of 1.0, 1.7, and 3.5 for FAUs prepared in this study, and 1.2 and 2.4 for commercial specimens. In addition, ratios of 18 and 200 were determined for FER and MOR treated in the present study.

The amount of DEP adsorbed on each FAU was estimated by the following method: weights of DEP adsorbed on FAU and the silicon powder were recorded individually, and then both FAU and silicon powder were mixed well. A part of the mixed sample was inserted into an NMR tube, and ^{1}H MAS NMR spectra were obtained with a MAS rate of 30 kHz. It is assumed that the area under a peak in the NMR signal is proportional to the amount of H atoms in the tube. Therefore, the ratio between the signal areas of DEP and silicon powder gives the amount of DEP adsorbed on a unit weight of FAU. We additionally measured the relaxation times of ^{1}H MAS NMR signals. Spin-lattice relaxation time (T_1) of the ^{1}H nucleus was obtained using an inversion recovery method. In this method, FID was accumulated as a function of τ in a π-τ-$\pi/2$ pulse sequence.

In order to identify the NMR signals, ^{1}H NMR spectra of DEP dissolved in D_2O solvent were obtained using the same apparatus (this spectrometer can be used to analyze samples both in solution and in the solid state by changing the probe). Chemical-shift (CS) values of the ^{1}H nucleus were calibrated by employing the CS value of the ^{1}H signal in D_2O (99.8%-*d*). CS values of DEP were also simulated using the MP2/cc-pVDZ function in a Gaussian 03 program. Before the CS estimation, atomic arrangements in DEP were optimized using the function B3LYP/6-311+G**. By applying the same processes to a tetramethylsilane (TMS) molecule and subtracting the isotropic value of the shielding tensors estimated in DEP from that of TMS, we obtained the simulated CS values.

3. Results and Discussions

Fig 1: ^{1}H NMR spectra of DEP solution filtered from porous FAU, FER, MOR, and MCM-41. These spectrawere obtained by adding 0.00 (black), 0.01 (green), 0.10 (blue), and 1.00 g (red line) of each porous materialinto 10.0 mL saturated DEP aqua solution (H_2O:D_2O = 9:1).

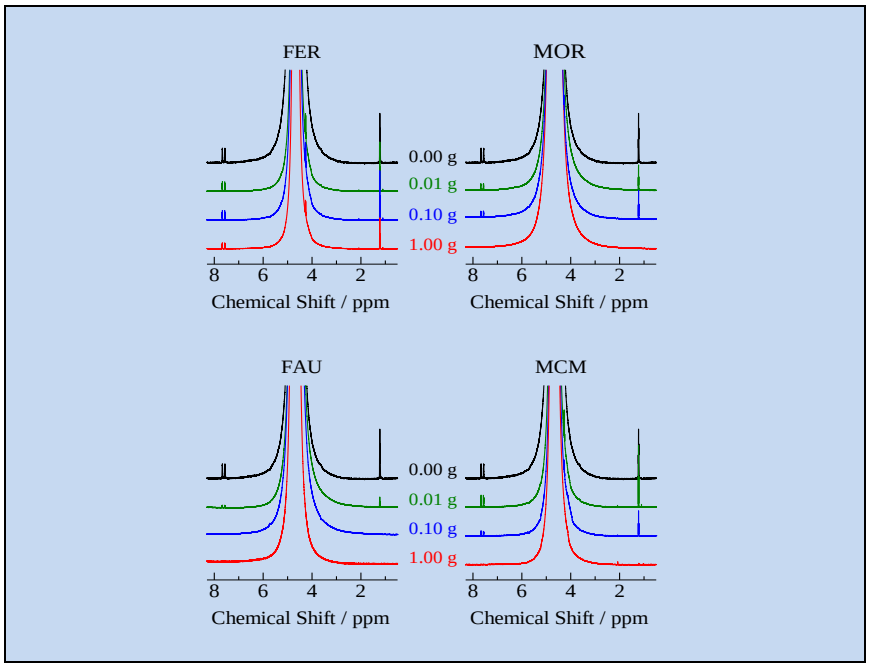

In order to estimate the amount of DEP adsorbed on the adsorbents (FAU, FER, MOR, and MCM-41), the following method was used: 0.01, 0.10, and 1.00 g of adsorbents were each added to 10.0 mL DEP saturated solution (H_2O:D_2O = 9:1). After stirring each solution for 24 h at room temperature, the solutions were filtered. ^{1}H NMR spectra of the filtrates are displayed in Fig. 1. In order to identify the peaks in the NMR spectra, DFT estimations were performed using an MP2/cc-pVDZ function. The results and assignments are shown in Table 1. Based on our CS simulation, the largest peak recorded at ~4.7 ppm in the ^{1}H NMR spectra can be attributed to H atoms in water. Subtracting the peak areas of the filtrates from those of the DEP saturated solution, removing ratios were obtained, as listed in Table 2. From this result, it is concluded that FAU is desirable for eliminating DEP molecules from aqueous solutions compared to the other porous materials.

Table 1: Observed and Simulated ^{1}H NMR Chemical Shift Values of DEP

	-CH_3	-CH_2-	*m*-	*o*-
Observed values / ppm	1.33	4.38	7.67	7.78
Calculated values / ppm	1.35	4.16	7.14	7.80

Table 2: Removing Ratios of DEP from 10.0 mL Saturated Aqueous Solution			
Mass of Adsorbents	**0.01 g**	**0.10 g**	**1.00 g**
FAU	87.6%	93.2 %	100.0 %
FER	52.5%	65.3 %	100.0 %
MOR	33.2%	33.6 %	72.5%
MCM-41	15.7%	56.7 %	99.1 %

In order to determine the amount of DEP adsorbed on the adsorbents, FER, MOR, FAU, and MCM-41, ^{1}H MAS NMR spectra of the residues were obtained, (Fig. 2). In this figure, the peak observed at 0.12 ppm is the internal reference silicon powder. Because the signals detected at ~1.3 and 7.7 ppm were assigned to the H atoms of -CH_3 and the benzene ring in DEP molecules adsorbed on each porous material, respectively, it can be concluded that DEP molecules were adsorbed on each adsorbent. The largest peak recorded at ~4.7 ppm can be linked to the H atoms of water molecules in the materials. In the case of FER, the water signal was detected at 3.8 ppm. This difference suggests that water molecules are adsorbed on the FER framework by weak interactions compared to the other porous materials treated in this study (In general, ^{1}H NMR CS becomes smaller if the electron density at the H atom is larger. Since water molecules are adsorbed on the cations in zeolites, small CS values of water molecules result in weak interaction). In the case of MCM-41, the signals recorded at 2.3 and 3.8 ppm were also observed without DEP, therefore, these lines can be assigned to H atoms of MCM-41 framework. Based on the peak intensities of DEP recorded at around 1.3 and 7.7 ppm in Fig. 2 and the removing ratios listed in Table 2, it can be concluded that FAU is a more suitable material for eliminating DEP from the water system than FER, MOR, and MCM-41.

Fig. 2: ^{1}H MAS NMR spectra of FAU, FER, MOR, and MCM-41 after filtration from DEP saturated aqueous solution. The spectra were recorded using a MAS rate of 30 kHz at room temperature.

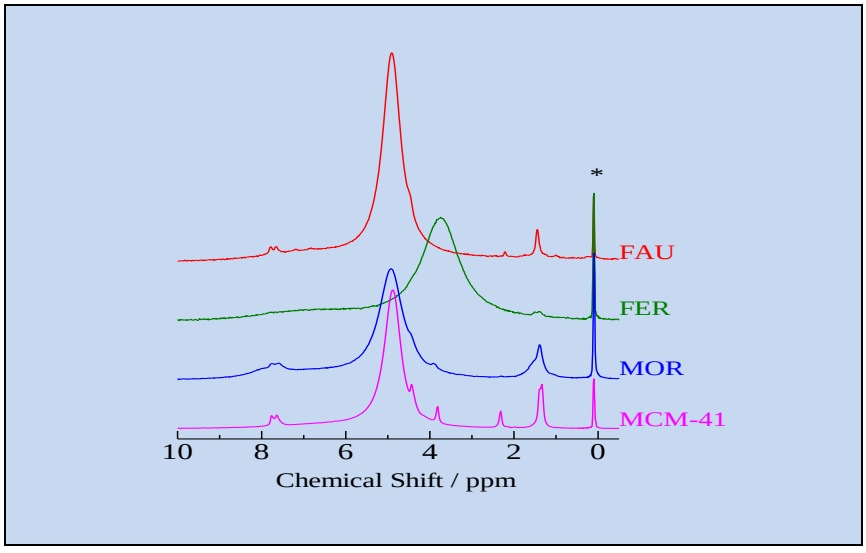

FAUs can be prepared with various Si/Al ratios, and in addition, they can be ion-exchanged by alkali-metal cations. Therefore, in the next step, 25 kinds of FAU (five Si/Al ratios of 1.0, 1.2, 1.7, 2.4, 3.5 and five cations Li^+, Na^+, K^+, Rb^+, Cs^+) were treated to reveal the most suitable conditions for removing DEP from aqueous solutions and the adsorbed states of DEP in FAUs. Each ion-exchanged FAU (M*x*, 0.10 g) was added to 19, 43, and 129 mL of DEP saturated aqueous solutions, individually. After stirring for 24 h at room temperature, the solutions were filtered. ^{1}H MAS NMR spectra obtained from the residues are shown in Fig. 3. In these spectra, the peaks observed at 0.12 and ~4.7 ppm can be linked to the H atoms of silicon powder (internal reference) and water

molecules, respectively. The peaks in the NMR spectra show that the amount of DEP adsorbed on the FAUs increases with their Si/Al ratios. In addition, the signal assigned to the H atoms of water is shifted to small CS values with increasing Si/Al ratios. This tendency has been explained by the increasing hydrophobicity of the zeolite surface [52]. Based on this fact, the observation that larger peak-areas of DEP were obtained for the NMR spectra of DEP(aq)-M*x* with larger x can be linked to the hydrophobicity of DEP in water. In order to analyze this quantitatively, DEP adsorbed ratios are plotted as a function of the CS value of water (Fig. 4). Here, the DEP adsorbed ratios were estimated by the following process: the weight ratio of DEP(aq)-M*x* to silicon powder in the NMR tube was recorded before obtaining the NMR spectra. Each signal area of $-CH_3$ and silicon powder observed in the spectra was estimated by fitting a Lorentz function, and a signal-area ratio of DEP/(silicon powder) was estimated. The DEP adsorbed ratios were finally calculated by dividing the signal-area ratio by the weight ratio for each FAU. Based on this figure, it is believed that the amount of adsorbed DEP is correlated to the hydrophobicity of FAUs. In this study, we checked the pH values of the DEP solutions after filtering the FAUs, because it is hypothesized that they affect the DEP adsorption. The result is displayed in Table 3. The pH value of the DEP saturated solution was 5.22 before the addition of FAUs, and increased upon adding FAUs. It is believed that this change is caused by a small amount of alkali-metal cations that were ion-exchanged and exuded into water. Although the pH values increase, large differences were not observed among FAUs, and no correlation was found between pH and the CS values and between the DEP adsorbed ratio and pH values. Therefore, it can be regarded that the hydrophobicity of the zeolite framework is strongly linked to DEP adsorption.

Fig. 3: ^{1}H MAS NMR spectra observed in the residues of M-type FAUs (M = Li, Na, K, Rb, Cs) with Si/Al ratios of 1.0, 1.2, 1.7, 2.4, and 3.5, after filtration from DEP saturated aqueous solution. The spectra were recorded using a MAS rate of 30 kHz at ambient temperature. In this observation, each FAU of 0.10 g was added into (a) 19 mL, (b) 43 mL, and (c) 129 mL of saturated solution.

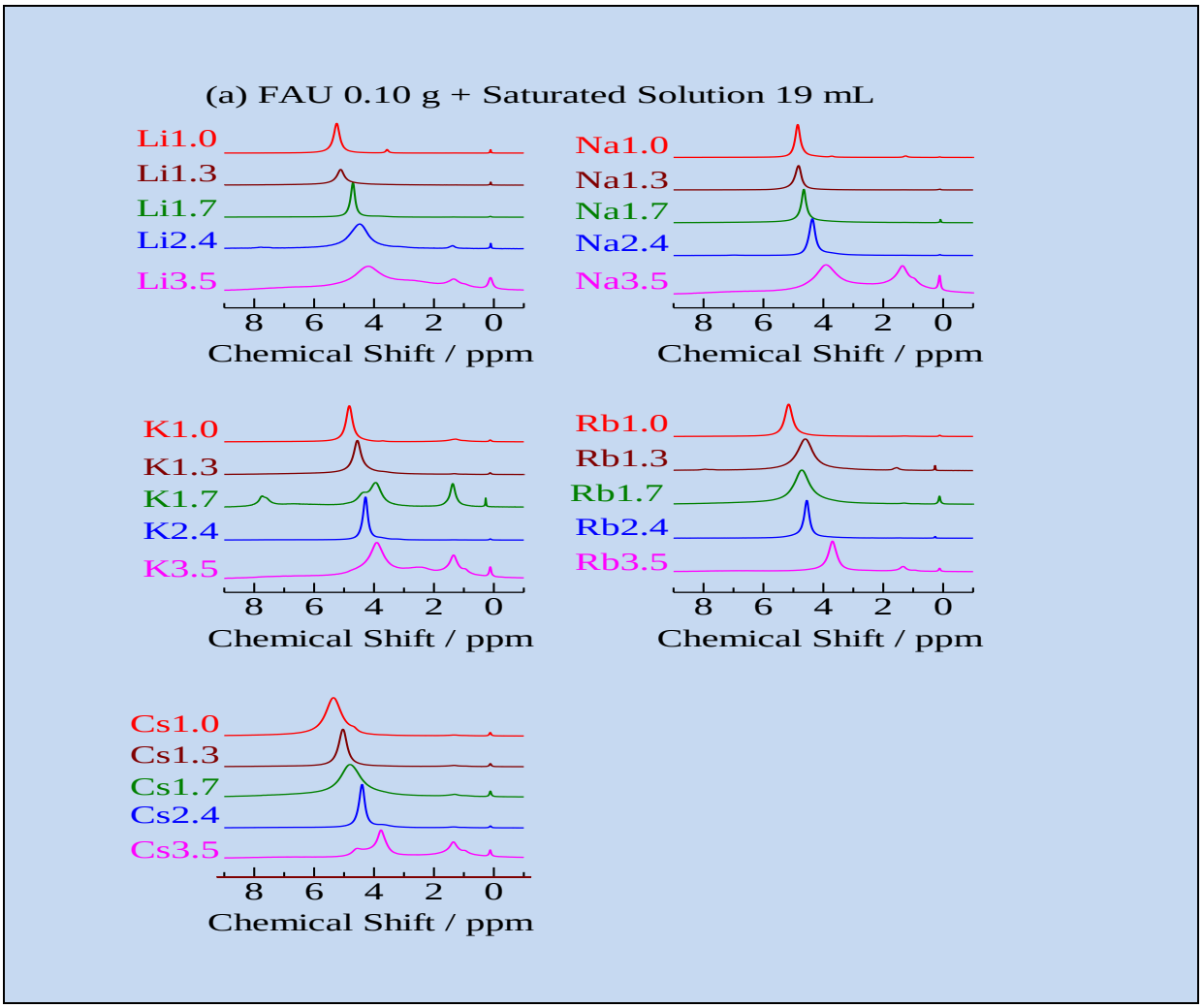

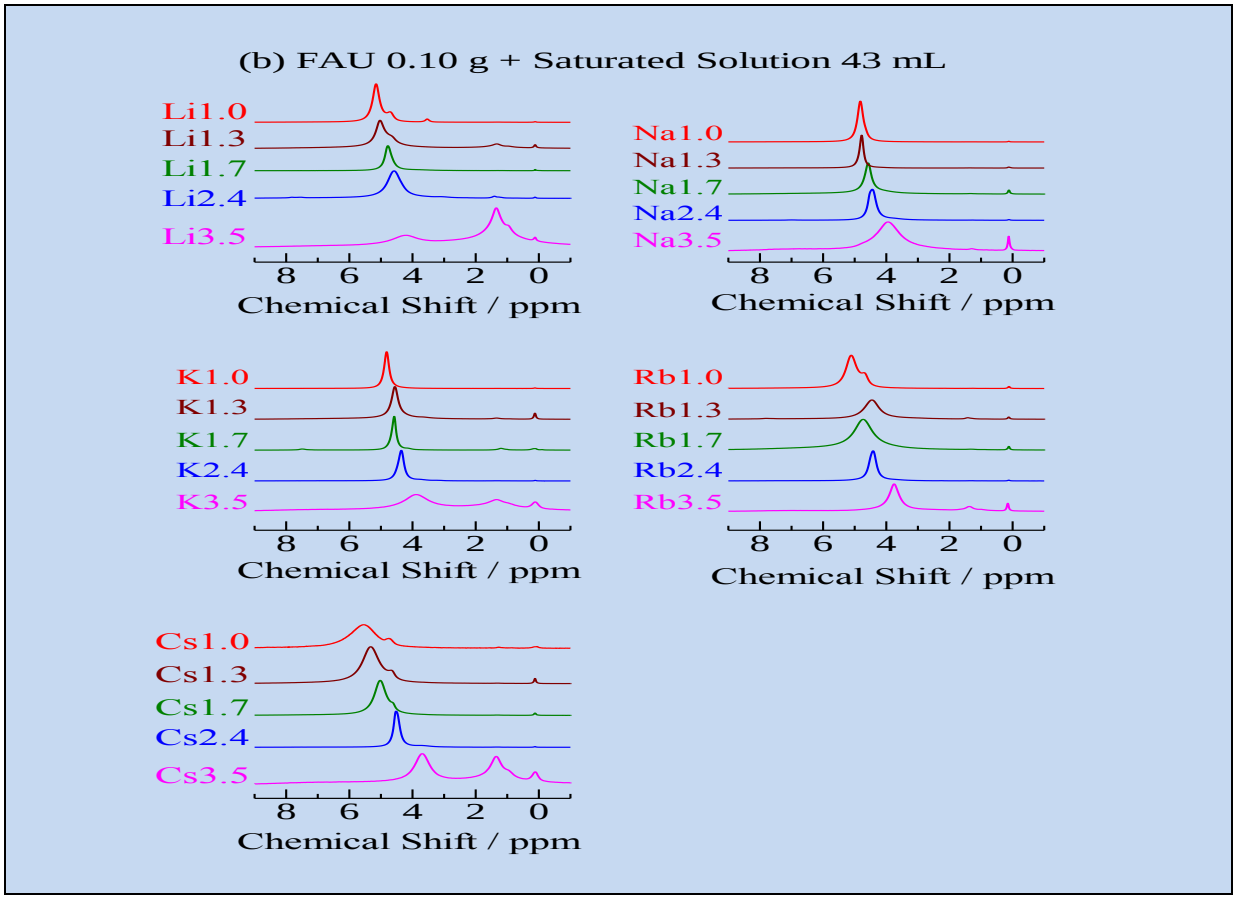
(b) FAU 0.10 g + Saturated Solution 43 mL
Li1.0
Li1.3
Li1.7
Li2.4
Li3.5
8 6 4 2 0
Chemical Shift / ppm
Na1.0
Na1.3
Na1.7
Na2.4
Na3.5
8 6 4 2 0
Chemical Shift / ppm
K1.0
K1.3
K1.7
K2.4
K3.5
8 6 4 2 0
Chemical Shift / ppm
Rb1.0
Rb1.3
Rb1.7
Rb2.4
Rb3.5
8 6 4 2 0
Chemical Shift / ppm
Cs1.0
Cs1.3
Cs1.7
Cs2.4
Cs3.5
8 6 4 2 0
Chemical Shift / ppm

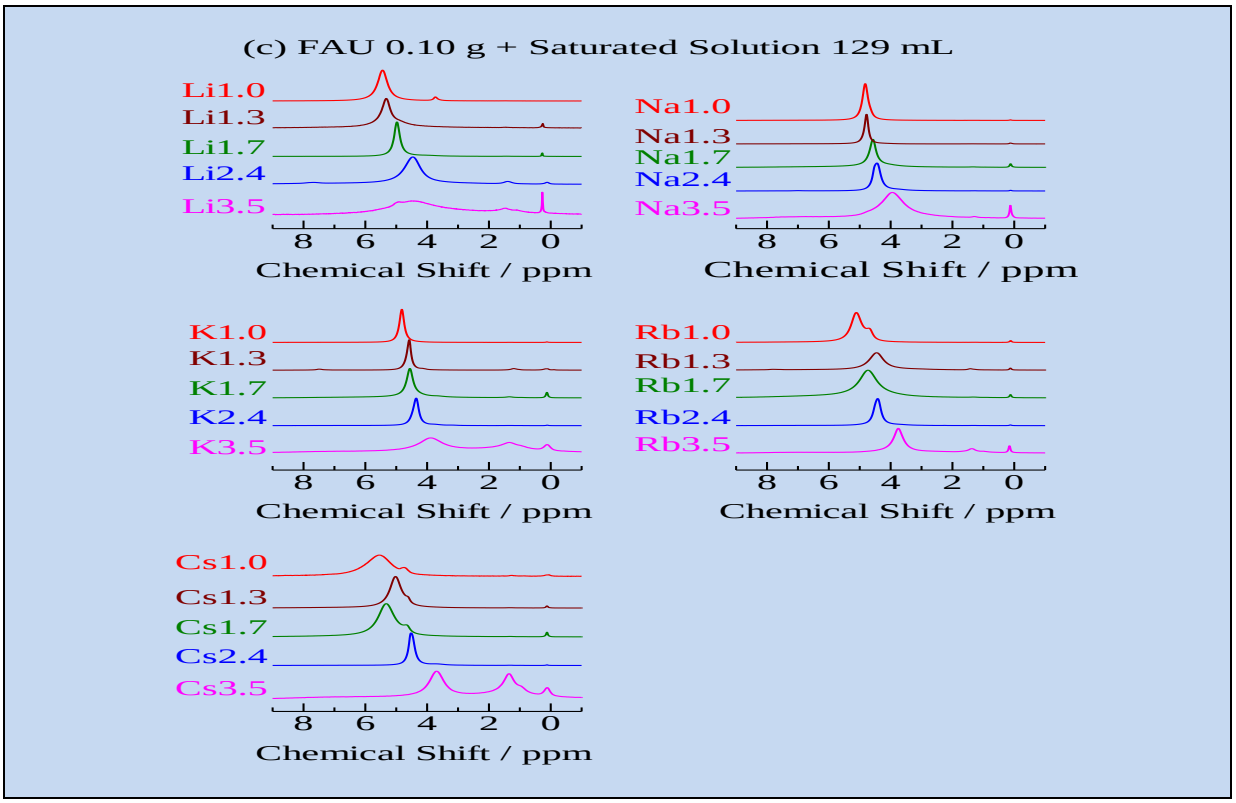
(c) FAU 0.10 g + Saturated Solution 129 mL
Li1.0
Li1.3
Li1.7
Li2.4
Li3.5
8 6 4 2 0
Chemical Shift / ppm
Na1.0
Na1.3
Na1.7
Na2.4
Na3.5
8 6 4 2 0
Chemical Shift / ppm
K1.0
K1.3
K1.7
K2.4
K3.5
8 6 4 2 0
Chemical Shift / ppm
Rb1.0
Rb1.3
Rb1.7
Rb2.4
Rb3.5
8 6 4 2 0
Chemical Shift / ppm
Cs1.0
Cs1.3
Cs1.7
Cs2.4
Cs3.5
8 6 4 2 0
Chemical Shift / ppm

Fig. 4. DEP adsorbed ratios as a function of chemical shift values of water molecules adsorbed on FAUs. Li, Na, K, Rb, and Cs-type FAUs are shown by red, orange, green, blue, and purple symbols, respectively, and Si/Al ratios of 1.0, 1.2, 1.7, 2.4, and 3.5 are displayed by closed circle, opened triangle, closed square, opened circle, and cross, respectively.

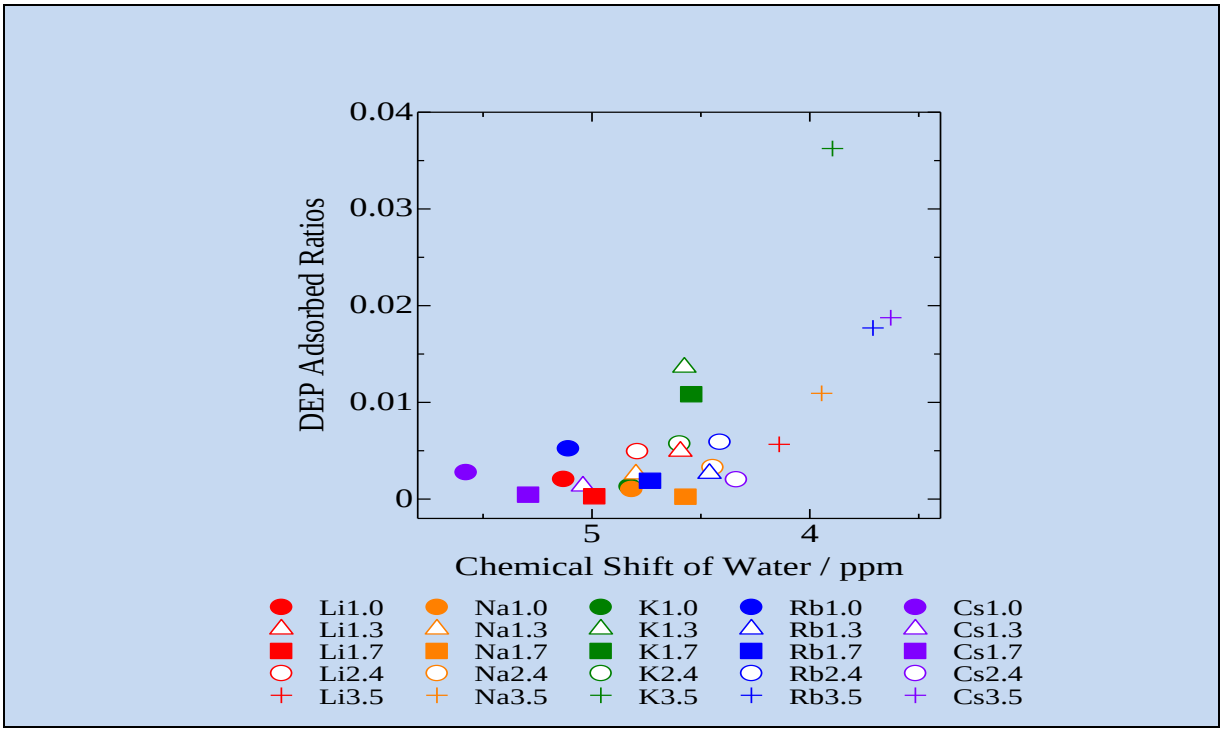

Table 3: pH Values of DEP Solution with FAUs. pH Value of DEP Saturated Solution was 5.22 Before Adding FAUs.

	1.0	1.2	1.7	2.4	3.5
Li	8.02	6.76	6.10	6.46	6.65
Na	7.76	6.81	5.31	6.73	6.78
K	5.96	6.19	7.00	6.89	6.77
Rb	6.91	6.85	6.38	6.87	6.69
Cs	5.81	6.92	6.78	6.70	6.74

In the case of FER and MOR, Si/Al ratios of 18 (FER) and 210 (MOR) were employed in this study, however, only a small amount of DEP adsorption was determined from the ^{1}H NMR spectra, as displayed in Table 2. This inconsistency can be explained by the pore size in each zeolite: the window size of a supercage is ~740 pm in FAUs; in contrast, it is ~430 and ~670 pm in FER and MOR, respectively. Since the molecular length and width of DEP was estimated to be about 960 and 660 pm by our DFT simulation, respectively, it is assumed that DEP molecules can perform translational motion in FAU, which is more difficult in FER and MOR. In the case of MCM-41, the window size of the channel is ~2 nm and the inner surface is composed of SiO_2 units. However, our results showed that FAU is more suitable for removing DEP from aqueous solutions compared to MCM-41, as shown in Table 2. In order to study this inconsistency, the surface area of adsorption was measured in the adsorbents. The results of N_2 adsorption isotherms are shown in Fig. 5. These line-shapes reveal that FAU, FER, and MOR show the type I adsorption curve, as defined by the IUPAC classification: N_2 molecules adsorb in the micro- and macro-pores of these materials over a range of low and high relative pressures, respectively. In contrast, the N_2 adsorption isotherms of MCM-41 as a function of relative pressure can be classified as type IV. Therefore, there are mesopores in MCM-41. Based on these adsorption curves, specific surface-areas of 695, 35,

442, and 791 $m^2 \cdot g^{-1}$ were estimated for FAU, FER, MOR, and MCM-41, respectively. These data suggest that the adsorption ability of MCM-41 is greater than that of FAU. In general, it is known that there are several silanol (Si-OH) groups on the surface of MCM-41 as well as on FAUs. Therefore, it is hypothesized that the large channel radius of MCM-41 compared to the DEP molecule allows a coating of water molecules on the inner surface of MCM-41, resulting in high DEP mobility in the channel. In the case of FAUs, it has a suitable window-size for attaching DEP molecules in the supercage.

Fig. 5: N_2 Adsorption Isotherms of FAU (Red), FER (Green), MOR (Blue), and MCM-41 (Purple).

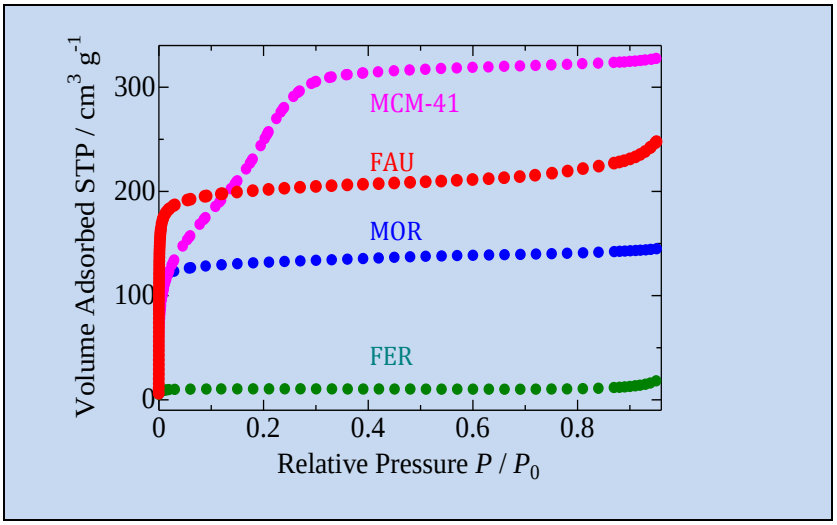

In order to reveal the adsorption states of the adsorbate on FAUs, liquid DEP was added into the FAUs (DEP is in a liquid state at ambient conditions) and ^{1}H MAS NMR spectra of the filtrates (DEP(l)-M*x*) were measured. The results are shown in Fig. 6, in which the peaks of water molecules were observed. In addition, large signal intensities of DEP molecules were detected in FAUs except for x = 1.0, compared to those displayed in Fig. 3. Based on these results, it is concluded that (i) most water molecules are retained in FAUs (do not diffuse into the DEP liquid) and (ii) DEP can adsorb onto FAUs even if there are water molecules present in the super cages. In addition, two kinds of -CH_3 peaks were detected at ~1.1 and 1.5 ppm in Li2.4, K2.4, Cs2.4, etc. The intensity of the signal at 1.5 ppm was drastically reduced with decreasing Si/Al ratios. A similar tendency was observed at ~7.5 and 8.0 ppm (these signals can be assigned to the H atoms of the benzene ring). Based on the reducing ratio of signal intensity as a function of Si/Al ratios, the peaks recorded at ~1.1 and 7.5 ppm can be assigned to the same DEP molecules, and the other set at 1.5 and 8.0 ppm corresponds to the other DEP molecules adsorbed on FAUs. From this it is believed that there are two kinds of adsorbed sites for DEP molecules in FAUs. The ^{1}H MAS NMR line-widths observed at 1.5 and 8.0 ppm were larger than those of the others at 1.1 and 7.5 ppm, implying that the former peaks corresponding to strongly adsorbed DEP molecules, while the latter signals correspond to weakly bound molecules, which perform large amplitude motions e.g. isotropic rotation, at the site. Since DEP molecules show hydrophobicity, they prefer to adsorb on hydrophobic sites (cation-free sites) on the framework. It is reported that there are three kinds of alkali metal ion sites (Site I, II, and III) in FAUs [35-42]: Site I is located in the hexagonal prism and the soda lite cage, therefore, this site contributes little to DEP adsorption (no DEP molecule can be inserted into the framework). In contrast, Site III, II, and III' are found on four- and six-membered ring, and windows (twelve-ring), respectively. It has also been reported that the population of cations on Sites III and III' increase with decreasing Si/Al ratios, although those on Site II are independent of the Si/Al ratios (over a range of Si/Al < 5) [35-42]. This suggests that DEP molecules prefer to adsorb on the four-ring site (corresponding to 1H NMR signal observed at 1.5 and 8.0 ppm) rather than on the other sites, e.g. window (joining space of two super cages) or/and center of the supercage (corresponding to 1.1 and 7.5 ppm). This model can explain the entire dataset. The signal intensities recorded at 1.5 and 8.0 ppm increased with increasing Si/Al ratios. The increasing Si/Al ratio results in decreasing concentration of the alkali-metal ion on four-membered ring sites in FAUs. The signal intensities observed at 1.1 and 7.5 ppm increased with decreasing Si/Al ratios. This result is also illustrated by assuming that there is limit on the number of DEP molecules in the supercage. DEP prefers to adsorb on the four-membered ring sites. However, if those sites are occupied by M^+ cations, DEP can adsorb onto the secondary stable site (center of supercage or/and window). In the case of Si/Al = 1.0, entire sites are occupied by cations, and little DEP can link to FAUs.

Fig. 6: ^{1}H MAS NMR spectra observed in the residues of M-type FAUs (M = Li, Na, K, Rb, Cs) with Si/Al ratios of 1.0, 1.2, 1.7, 2.4, and 3.5, after filtration from DEP in a liquid state. The signals were recorded using a MAS rate of 30 kHz at room temperature.

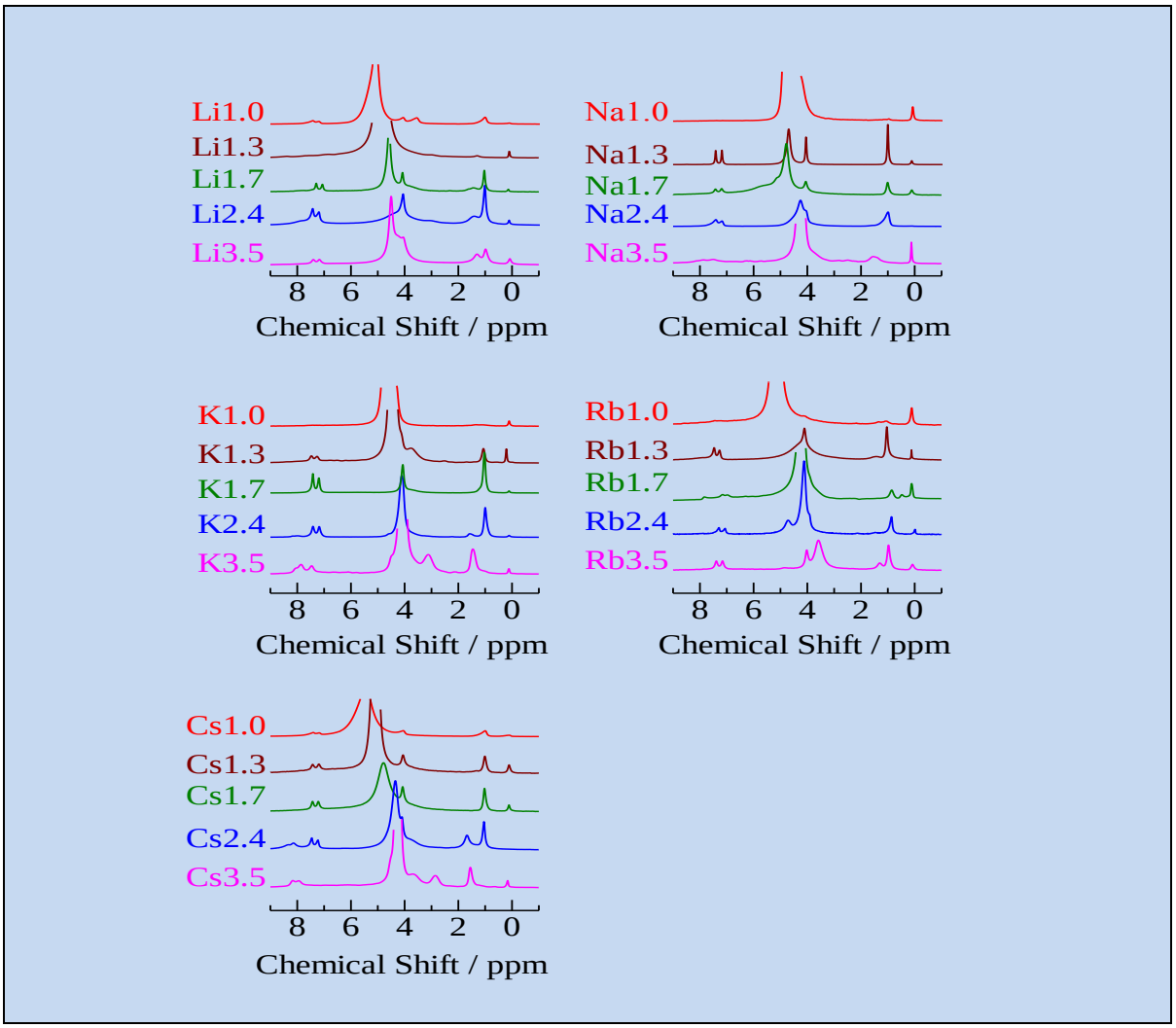

In order to reveal the dynamic difference between the two kinds of DEP molecules in FAU, ^{1}H MAS NMR T_1 measurements were carried out. ^{1}H MAS NMR spectra are plotted in Fig. 7 as a function of τ, which is the time between π and π/2 pulses in an inversion-recovery pulse-sequence. In the case of the inversion recovery method, the T_1 value is related to the signal area of $M_z(\tau)$ at each τ value by the following equation [67]:

$$M_z(\tau) = M_{eq}\left[1 - 2\exp\left(-\frac{\tau}{T_1}\right)\right]$$

Here, M_{eq} is the peak area in a thermal equilibrium state (corresponding to infinite τ). In this figure, fast recovery was observed at ~4 ppm (water signal), whereas DEP signals were recovered at $\tau > 0.75$ s. By fitting the above equation to each signal area recorded, T_1 values of 0.16, 1.43, and 1.78 s were obtained for water and DEP adsorbed on the secondary site and four-membered ring site, respectively. Based on these T_1 values, it can be considered that water molecules in the FAU perform fast motion rather than the molecular motions of DEP adsorbed on the FAUs, and molecular motions of DEP located on four-member ring are slightly restricted compared to those on the center of the supercage or/and window.

Fig. 7: ^{1}H MAS NMR spectra observed in the residues of K-type FAUs with the Si/Al ratio of 2.4 as a function of interval time (τ) between π and π/2 pulses (inversion recovery method). The signals were recorded with the MAS rate of 30 kHz at room temperature. *: internal reference of silicon powder (0.12 ppm)

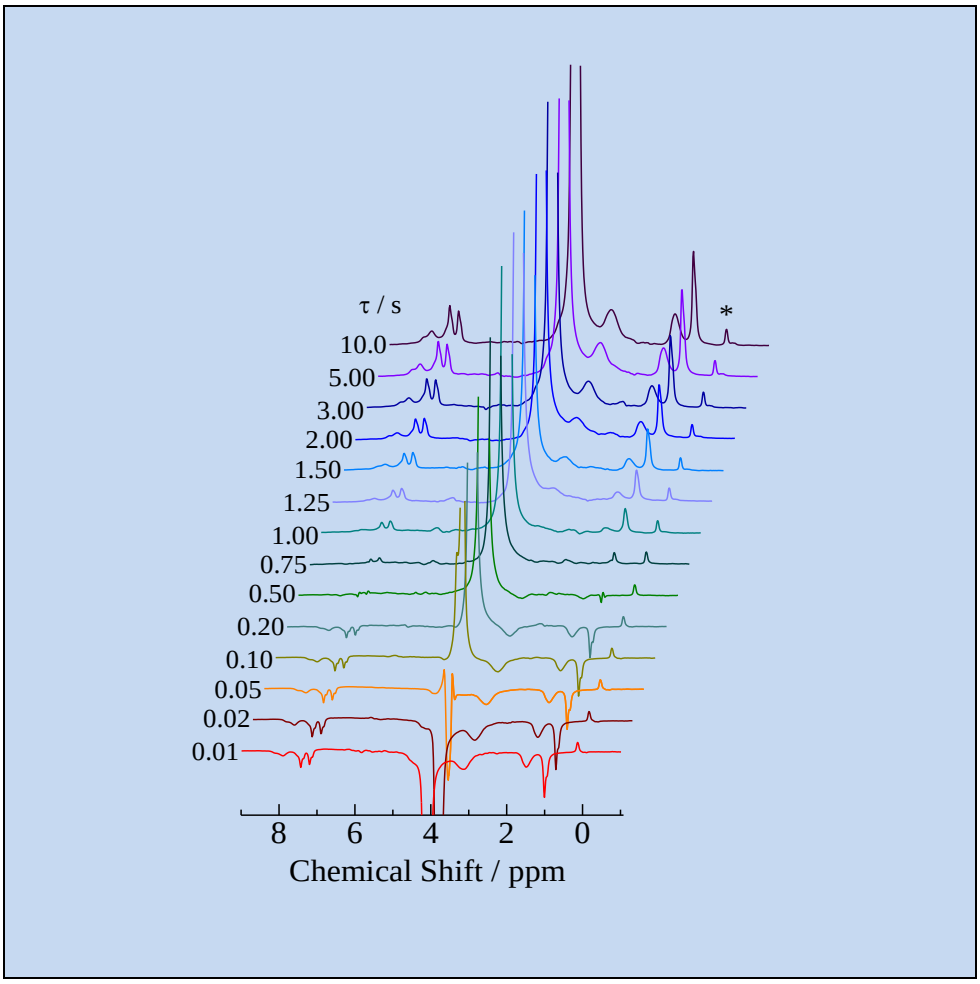

4. Conclusion

We treated FAU, FER, MOR, and MCM-41, in order to investigate DEP filtration from an aqueous system. ^{1}H NMR measurements showed that FAU was suitable for removing DEP from aqueous solutions compared to the other porous materials FER, MOR, and MCM-41. In addition, our ^{1}H NMR spectra revealed that a larger DEP adsorption was observed in FAU with higher Si/Al ratios. Since the signal attributed to H atoms from the water adsorbed on FAU was recorded at lower CS values with higher Si/Al ratios, it is believed that hydrophobic FAU is desirable for removing DEP from aquatic environments. Compared to alkali metal ions, the water peak was detected at low CS values in K- and Rb-type FAUs and a large amount of DEP adsorption was obtained in these FAUs. Based on these results, we conclude that DEP was effectively eliminated from water systems using K- and Rb-type FAUs with a Si/Al ratio of 3.5. We also revealed that DEP molecules could be adsorbed on the four-membered ring and the center of the supercage or/and window (the former being the preferred site for DEP). Since porous materials are frequently present in soils and attached to water systems such as rivers, and lakes, this study also showed that DEP could adsorb on soil particles in water systems.

Acknowledgements

The authors are grateful to Nissan Chemical Industries, Ltd., TORAY, and Tosoh for providing Snotecs 40, silicon powder EP-2600, and FAUs with Si/Al ratio of 1.2 and 2.4, respectively. This work was partly supported by a Grant in Support of Promotion of Research at Yokohama City University.

References

[1] Leyder, F., Boulanger, P. (1983). Ultraviolet adsorption, aqueous solubility and octanol–water partition for several phthalates. *Bull. Environ. Contam. Toxicol.*, *30*, 152–157.

[2] Clara, M, Windhofer, G, Hartl, W, Braun, K, Simon, M, Gans, O, Scheffknecht, C, Chovanec, A. (2010). Ocurrence of phthalates in surface runoff, untreated and treated wastewater and fate during wastewater treatment. *Chemosphere*, *78*, 1078–84.

[3] Liang, DW, Zhang, T, Fang, HP, He, J. (2008). Phthalates biodegradation in the environment. *Appl. Microbiol. Biotechnol.*, *80*, 183–198.

[4] Staples, CA, Peterson, DR, Parkerton, TF, Adams, WJ. (1997). The environmental fate of phthalate esters. *Chemosphere*, *35* 667–749.

[5] Pant, N, Shukla, M, Patel, DK, Shukla, Y, Mathur, N, Gupta, YK, Saxena, DK. (2008). Correlation of phthalate exposures with semen quality. *Toxicology and Applied Pharmacology*, *231*, 112–116.

[6] Zhao, XK, Yang, GP, Wang, YJ. (2004). Adsorption of dimethyl phthalate on marine sediments. *Water, Air, and Soil Pollution*, *157*, 179–192.

[7] Barnabé, S, Beauchesne, I, Cooper, DG, Nicell, JA. (2008). Plasticizers and their degradation products in the process streams of a large urban physicochemical sewage treatment plant. *Water Research*, *42*, 153–162.

[8] Huang, M, Li, Y, Gu, G. (2010). Chemical composition of organic matters in domestic wastewater. *Desalination*, *262*, 36–42.

[9] Sipma, J, Osuna, B, Collado, N, Monclus, H, Ferrero, G, Comas, J, Roda, IR. (2010). Comparison of removal of pharmaceuticals in MBR and activated sludge system. *Desalination*, *250*, 653–659.

[10] Simmchen, J, Ventura, R, Segura, J. (2012). Progress in the removal of di-[2-ethylhexyl]-phthalate as plasticizer in blood bags. *Transfusion Medicine Reviews*, *26*, 27–37.

[11] Venkata, MS, Shailaja, S, Rama, KM, Sarma, PN. (2007). Adsorptive removal of phthalate ester (di-ethylphthalate) from aqueous phase by activated carbon: a kinetic study. *Journal of Hazardous Materials*, *146*, 278–282.

[12] Peakall, DB. (1975). Phthalate esters: occurrence and biological effects. *Residue Rev.*, *54*, 1–41.

[13] Michalowicz, J, Duda, W. (2007). Phenol—sources and toxicity. *J. Environ. Stud.* , *6.3*, 347–362.

[14] Kapanen, A, Stephen, JR, Bru¨ggemann, J, Kiviranta, A, White, DC, Ita¨vaara, M. (2007). Diethyl phthalate in compost: ecotoxicological effects and response of the microbial community. *Chemosphere*, *67*, 2201–2209.

[15] Pham, TTH, Tyagi, RD, Brar, SK, Surampalli, RY. (2011). Effect of ultrasonication and Fenton oxidation on biodegradation of bis(2-ethylhexyl) phthalate (DEHP) in wastewater sludge. *Chemosphere*, *82*, 923–928.

[16] Özer, ET, Gücer, S. (2011). Determination of some phthalate acid esters in arti-ficial saliva by gas chromatography mass spectrometry after activated carbon enrichment. *Talanta*, *84*, 362–367.

[17] Julinová, M, Slavík, R. (2012). Removal of phthalates from aqueous solution by different adsorbents: a short review. *Journal of Environmental Management*, *94*, 13–24.

[18] Oliveira, TF, Cagnon, B, Fauduet, H, Licheron, M, Chedeville, O. (2012). Removal of Diethyl Phthalate from Aqueous Media by Adsorption on Different Activated Carbons: Kinetic and Isotherm Studies. *Separation Science and Technology*, *47*, 1139–1148.

[19] Zhang, W, Xu, Z, Pan, B, Hong, C, Jia, K, Jiang, P, Zhang, Q, Pan, B. (2008). Equilibrium and heat of adsorption of diethyl phthalate on heterogeneous adsorbents. *J. Colloid Interface Sci*. *325*, 41–47.

[20] Xu, Z., Zhang, W, Pan, B, Lv, L, Jiang, Z. (2011). Treatment of aqueous diethyl phthalate by adsorption using a functional polymer resin. *Environ. Technol.*, *32*, 145–153.

[21] Özer, ET, Osman, B, Kara, A, Besirli, N, Gücer, S, Sözeri, H. (2012). Removal of diethyl phthalate from aqueous phase using magnetic poly(EGDMA–VP) beads. *Journal of Hazardous Materials*. *229– 230*, 20– 28.

[22] Yu, X, Wei, C, Ke, L, Wu, H, Chai, X, Hu, Y. (2012). Preparation of trimethylchlorosilane-modified acid vermiculites for removing diethyl phthalate from water, *Journal of Colloid and Interface Science*, *369*, 344–351.

[23] Shi, Q, Li, A, Zhou, Q, Shuang, C, Li, Y. (2014). Removal of diethyl phthalate from aqueous solution using magnetic iron–carbon composite prepared from waste anion exchange resin. *Journal of the Taiwan Institute of Chemical Engineers*, *45*, 2488–2493.

[24] Okolia, CP, Adewuyi, GO, Zhang, Q, Diagboya, PN, Guo, Q. (2014). Mechanism of dialkyl phthalates removal from aqueous solution using γ-cyclodextrin and starch based polyurethane polymer adsorbents. *Carbohydrate Polymers*, *114*, 440–449.

[25] Prasad, B, Suresh, S. (2012). Biodegradation of dimethyl phthalate, diethyl phthalate, dibutyl phthalate and their mixture by Variovorax sp, *Int. J. Environ. Sci. Dev*. *3*, 283–8.

[26] Boonnorat, J, Chiemchaisri, C, Chiemchaisria, W. (2014). Yamamoto, K., Removals of phenolic compounds and phthalic acid esters in landfillleachate by microbial sludge of two-stage membrane bioreactor. *Journal of Hazardous Materials*, *277*, 93–101.

[27] Jin, OK, Sook, YY, Kang, JW. (2006). Application of ozone, UV and ozone/UV processes to reduce diethylphthalate and its estrogenic activity. *Science of the Total Environment*, *367*, 681–693.

[28] Vazquez-Gomez, L, de Battisti, A, Ferro, S, Cerro, M, Reyna, S, Martı´nez-Huitle, CA, Quiroz, MA. (2012). Anodic Oxidation as Green Alternative for Removing Diethyl Phthalate from Wastewater Using Pb/PbO_2 and Ti/SnO_2 Anodes. *Clean – Soil, Air, Water*, *40*, 408–415.

[29] Soo, OB, Jung, JY, Jin, OY, Sook, Y, Kang, JW. (2006). Application of ozone, UV and ozone/UV processes to reduce diethyl phthalate and its estrogenic activity. *Science of the Total Environment*, *367*, 681–693.

[30] Oliveira, TF, Chedeville, O, Fauduet, H, Cagnon, B. (2011). Use of ozone/activated carbon coupling to remove diethyl phthalate from water: influence of activated carbon textural and chemical properties. *Desalination*, *276*, 359–365.

[31] Castillo, NAM, Pe´rez, RO, Ramos, RL, Polo, MS, Utrilla, JR, Dı´az, JDM. (2013). Removal of diethyl phthalate from water solution by adsorption, photo-oxidation, ozonation and advanced oxidation process (UV/H_2O_2, O_3/H_2O_2 and O_3/activated carbon). *Sci Total Environ*, *442*, 26–35.

[32] Shao, L, Ren, Z, Zhang, G, Chen, L. (2012). Facile synthesis, characterization of a $MnFe_2O_4$/ activated carbon magnetic composite and its effectiveness in tetracycline removal. *Mater Chem Phys.*, *135*, 16–24.

[33] Na, S, Ahn, YG, Cui, M, Khim, J. (2012), Significant diethyl phthalate (DEP) degradation by combined advanced oxidation process in aqueous solution. *J. Environ. Manage.*, *101*, 104–10.

[34] Baerlocher, C, McCusker, LB, Olson, DH. (2007). *Atlas of Zeolite Framework Types*, 6th ed. Elsevier: New York.

[35] Vitale, G, Mellot, CF, Bull, LM, Cheetham, (1997). K. Neutron Diffraction and Computational Study of Zeolite NaX: Influence of SIII‘ Cations on Its Complex with Benzene. *J. Phys. Chem. B*, *101*, 4559-4564.

[36] Beauvais, C, Boutin, A, Fuchs, AH. (2004). A Numerical Evidence for Nonframework Cation Redistribution Upon Water Adsorption in Faujasite Zeolite. *ChemPhysChem*., *5*, 1791-1793.

[37] Beauvais, C, Boutin, A, Fuchs, AH. (2005). Adsorption of water in zeolite sodium-faujasite: A molecular simulation study. *C. R. Chim.*, *8*, 485-490.

[38] Lella, AD, Desbiens, N, Boutin, A, Demachy, I, Ungerer, P, Bellat, JP, Fuchs, A. (2006). Molecular simulation studies of water physisorption in zeolites, *Phys. Chem. Chem. Phys.*, *8*, 5396-5406.

[39] Shirono, K, Endo, A, Daiguji, H. (2005). Molecular Dynamics Study of Hydrated Faujasite-Type Zeolites. *J. Phys. Chem. B.*, *109*, 3446-3453.

[40] Coasne, AB, Maurin, G, Henn, F, Jeffroy, M, Boutin, A. (2009). Cation Behavior in Faujasite Zeolites upon Water Adsorption: A Combination of Monte Carlo and Molecular Dynamics Simulations. *J. Phys. Chem. C.*, *113*, 10696-10705.

[41] Abrioux, C, Coasne, B, Maurin, G, Henn, F, Boutin, A, Lella, AD, Fuchs, AH. (2008). A molecular simulation study of the distribution of cationin zeolites. *Adsorption.*, *14*, 743-753.

[42] Zhu, L, Seff, K. (1999). Reinvestigation of the Crystal Structure of Dehydrated Sodium Zeolite X. *J. Phys. Chem. B*, *103*, 9512-9518.

[43] Semmer-Herle´dan, V, Heeribout, L, Batamack, P, Dore´mieux-Morin, C, Fraissard, J, Gola, A, Benazzi, E. (2000). Comparison of the acid strength of dealuminated H-faujasites determined by ^1H NMR after water adsorption. *Microporous Mesoporous Mater.*, *34*, 157-169.

[44] Freude, D, Hunger, M, Pfeifer, H. (1982). Study of brønsted acidity of zeolites using high-resolution proton magnetic resonance with magic-angle spinning. *Chem. Phys. Lett.*, *91*, 307-310.

[45] Freude, D, Hunger, M, Pfeifer, H, Schwieger, W. (1986). ^{1}H MAS NMR studies on the acidity of zeolites. *Chem. Phys. Lett.*, *128*, 62-66.

[46] Freude, D, Kilinowski, J, Hamdan, H. (1988). Solid-state NMR studies of the geometry of brønsted acid sites in zeolitic catalysts. *Chem. Phys. Lett.*, *149*, 355-362.

[47] Morita, T, Honda, H, Katayama, T, Tanaka, S, Ishimaru, S. (2014). Cation-Type Dependences of ^{1}H and ^{29}Si MAS NMR Chemical Shifts and Desorption Temperatures of Water Molecules in Faujasite-Type Zeolites. *Int. Res. J. Pure and Applied Chem.*, *4*, 638-655.

[48] Simoncic, P, Armbruster, T. (2004). Peculiarity and defect structure of the natural and synthetic zeolite mordenite: A single-crystal X-ray study. *Am. Mineral.*, *89*, 421–431.

[49] Dyer, A, Singh, AP. (1988). Effect of cation exchange on heat of sorption and catalytic activity of mordenties. *Zeolites*, *8*, 242-246.

[50] Bajpai, PK. (1986). Synthesis of mordenite type zeolite. *Zeolites*, *6*, 2-8.

[51] Maxwell, IE, Stork, WHJ, von Bekkum, H, Flanigen, EM, Jonsen, JC (Eds.). (1991). *Introduction to Zeolite Science and Practice*. Elsevier, Amsterdam, p.71.

[52] Fernandes, LD, Monteiro, JLF, Sousa-Aguiar, EF, Martinez, A, Corma, A. (1998). Ethylbenzene hydroisomerization over bifunctional zeolite based catalysts: The influence of framework and extraframework composition and zeolite structure. *J. Catal.*, *177*, 363-77.

[53] Vaughan, PA. (1966). The crystal structure of the zeolite ferrierite. *Acta cryst.*, *21*, 983–990.

[54] de Jong, KP, Mooiweer, HH, Buglass, JG, Maarsen, PK. (1997). Activation and deactivation of the zeolite ferrierite for olefin conversions. *Stud. Surf. Sci. Catal.*, *111*, 127–138.

[55] Houzvicka, J, Ponec, V. (1996). Skeletal isomerisation of *n*-butene on phosphorus containing catalysts. *Appl. Catal. A*, *145*, 95–108.

[56] Kim, WG, Kim, JH, Ahn, BJ, Seo, G. (2001). The Skeletal Isomerization of C4-C7 1-Olefins over Ferrierite and ZSM-5 Zeolite Catalysts. *Korean J. Chem. Eng.*, *18*, 120-126.

[57] Bordiga, S, Palomino, GT, Paze, C, Zecchina, A. (2000). Vibrational spectroscopy of H_2, N_2, CO and NO adsorbed on H, Li, Na, K-exchanged ferrierite. *Microporous Mesoporous Mater.*, *34*, 67–80.

[58] Nachtigall, P, Bludsky, O, Grajciar, L, Nachtigallova, D, Delgado, MR, Arean, CO. (2009). Computational and FTIR spectroscopic studies on carbon monoxide and dinitrogen adsorption on a high-silica H-FER zeolite. *Phys. Chem. Chem. Phys.*, *11*, 791–802.

[59] Bulanek, R, Frolich, K, Frydova, E, Cicmanec, P. (2010). Microcalorimetric and FTIR Study of the Adsorption of Carbon Dioxide on Alkali-Metal Exchanged FER Zeolites. *Top. Catal.*, *53*, 1349–1360.

[60] Vinu, A, Hossain, KZ, Ariga, K. (2005). Recent Advances in Functionalization of Mesoporous Silica. *J. Nanosci. Nanotechnol.*, *5*, 347-75.

[61] Jana, S, Dutta, B, Honda, H, Koner, S. (2011). Mesoporous silica MCM-41 with rod-shaped morphology: Synthesis and characterization. *Applied Clay Science*, *54*, 138–143.

[62] Lee, YY, Wu, KCW. (2012). Conversion and kinetics study of fructose-to-5-hydroxymethylfurfural (HMF) using sulfonic and ionic liquid groups bi-functionalized mesoporous silica nanoparticles as recyclable solid catalysts in DMSO systems. *Phys. Chem. Chem. Phys.*, *14*, 13914-13917.

[63] Peng, WH, Lee, YY, Wu, C, Wu, KCW. (2012). Acid–base bi-functionalized, large-pored mesoporous silica nanoparticles for cooperative catalysis of one-pot cellulose-to-HMF conversion. *J. Mater. Chem.*, *22*, 23181-5.

[64] Ariga, K, Yamauchi, Y, Rydzek, G, Ji, Q, Yonamine, Y, Wu, KCW, Hill, JP. (2014). Layer-by-layer Nanoarchitectonics: Invention, Innovation, and Evolution. *Chem. Lett.*, *43*, 36-68.

[65] Suzue, A, Honda, H, Kadokura, M, Tanaka, S, Tukada, H. (2014). Investigation of New Cooling Systems Based on Complexes of Temperature-Responsive Poly(N-isopropylacrylamide) with Porous Materials. *Bull. Chem. Soc. Jpn.*, *87*, 1186-1194.

[66] Sasaki, T, Shimada, K, Tabata, H. (2007). A Study on Lead Adsorption Property of Synthesized Mesoporous Silica. *Ishikawa-ken Kogyo Shikenjo Kenkyu Hokoku*, *56*, 69-74.

[67] Gerstein, BC, Dybowski, CR. (1985). Transient Techniques in NMR of Solids, Academic Press : New York.